J Mater Sci (2011) 46:6932–6940
DOI 10.1007/s10853-011-5659-5

Thermal stability of cryomilled nanocrystalline aluminum containing diamantane nanoparticles

K. Maung · R. K. Mishra · I. Roy · L.-C. Lai · F. A. Mohamed · J. C. Earthman

Received: 4 April 2011 / Accepted: 24 May 2011 / Published online: 8 June 2011

Abstract The thermal stability of nanoscale grains in cryomilled aluminum powders containing 1% diamantane was investigated. Diamantane is a diamondoid molecule consisting of 14 carbon atoms in a diamond cubic structure that is terminated by hydrogen atoms. The nanostructures of the resulting cryomilled powders were characterized using both transmission electron microscopy (TEM) and X-ray diffraction (XRD) techniques. The average grain size was found to be on the order of 22 nm, a value similar to that obtained for cryomilled Al without diamantane. To determine thermal stability, the powders were heated in an inert gas atmosphere at constant temperatures between 423 and 773 K ($0.51T_m$ to $0.83T_m$) for exposure times of up to 10 h. The average grain size for all powders containing diamantane was observed to remain in the nanocrystalline range (1–100 nm) for all exposures and was generally less than half of that for cryomilled pure Al heated under the same conditions. The thermal stability data were found to be consistent with a grain growth model based on drag forces exerted by dispersed particles against grain boundary migration. The present findings indicate that the presence of diamantane results in a substantial increase in the thermal stability of nanoscale grains in Al.

K. Maung · R. K. Mishra · I. Roy · L.-C. Lai · F. A. Mohamed · J. C. Earthman (✉)
Department of Chemical Engineering and Materials Science, University of California, Irvine, CA 92697-2575, USA
e-mail: earthman@uci.edu

Present Address:
R. K. Mishra
M*Modal, 1710 Murray Avenue, Pittsburgh, PA 15217, USA

Present Address:
I. Roy
Schlumberger Reservior Completions, 14910 Airline Road, Building 45-2586, Rosharon, TX 77583, USA

Present Address:
L.-C. Lai
Department of IREAP, University of Maryland, Bldg. 223, Room. 1203B, Paint Branch Drive, College Park, MD 20742-3511, USA

Introduction

Nanocrystalline (NC) materials are defined as single- or multi-phase polycrystals with grain size less than 100 nm in at least one dimension [1–3]. Considerable evidence has indicated that nanocrystalline alloys may provide mechanical and electrical properties superior to those of their coarse-grained counterparts. This potential superiority results from the reduced dimensionality of nanometer-sized crystallite as well as from the numerous interfaces between adjacent crystallites [3]. A number of processing techniques are currently available to produce NC materials including inert gas condensation [4], rapid solidification [5], electro-deposition [6], sputtering [7], crystallization of amorphous phases [8], laser ablation [9], chemical processing [10], and ball milling [11]. Comparison of these methods in terms of cost and productivity demonstrates that ball milling is the most cost effective route capable of producing NC materials in a large quantity. During the milling process, extreme cyclic deformation is induced in the powders as they undergo repeated welding, fracturing, and rewelding. Thus, the resulting nanostructure is produced by structural decomposition of coarse grains as the result of severe plastic deformation [12].

Rapid and extensive grain growth generally occurs during elevated temperature consolidation of cryomilled powders undermining the significant progress that has been

achieved in the synthesis of nanocrystalline precursors. Nanoscale grains tend to be highly unstable in this regard as predicted by the Gibbs–Thomson equation [13]. Accordingly, recent studies have investigated ways in which the thermal stability of nanocrystalline microstructure might be enhanced. For example, added thermal stability for cryomilled nanostructures is attributed to the pinning of grain boundaries by an inherent dispersion of second-phase Al_2O_3, AlN, and Al_4C_3 particles that results naturally from the cryomilling process [14–16]. These dispersions are incoherent second-phase particles, highly stable at high temperatures and insoluble in matrix. At elevated temperatures, they can act as a barrier to the movement of grain boundaries [17, 18]. However, the aforementioned particles are not fully effective in some cases including those related to Al and its alloys, possibly due to the fact that their size and spacing can exceed 80 nm [16]. For example, the average grain size of the as-milled powders of 5083 Al was reported to be about 50 nm, and that when the as-milled powders were consolidated via hot isostatic pressing and extrusion, the average grain size increased to about 400 nm [18]. On this basis, it is desirable to explore additions that enhance the thermal stability of Al or its alloys beyond that achieved via the dispersion of second-phase particles that results naturally from the cryomilling process. One such approach is to disperse smaller and more closely spaced nanoscale particles onto the grain boundaries via the cryomilling process. Accordingly, it was the primary goal of this study to examine how the addition of diamantane nanoparticles to Al powder during cryomilling affects grain size stability upon thermal exposure.

Methods and materials

The nanoscale particles selected for addition to pure Al during cryomilling are diamantane diamondoid hydrocarbon molecules each consisting of a 14 C atom diamond cubic framework that is terminated by hydrogen atoms [19]. Diamantane was selected partly because its cage of C atoms is <2 nm in diameter and also because it is stable, strong, and rigid as a result of its diamond cubic structure. The diamantane diamondoids used in this study were obtained from Chevron Texaco Technology Ventures-Molecular Diamond Technologies (Richmond, CA). A 1 wt% addition of diamantane was used in this study to achieve a significant effect on grain boundary stability at elevated temperatures. The basis for this amount of diamantane addition is given in the following.

A treatment by Yamasaki [20] has shown that the volume fraction of grain boundaries in a nanocrystalline material can be approximated by

$$f_{gb} = 1 - \left(\frac{d-\delta}{d}\right)^3 \quad (1)$$

where d is the grain size and δ is the grain boundary thickness. Previous study on cryomilled CP Al powders yielded average grain sizes on the order of 40 nm [15] and a reasonable estimate of the grain boundary thickness for this study is 0.5 nm [21]. Substituting these values in Eq. 1, we obtain $f_{gb} = 0.04$. An amount of diamantane required to account for about half of this volume fraction was chosen because it should be sufficient to have a significant effect on grain growth while below the level that would form a continuous layer of diamantane at the boundaries which could be detrimental. The composition of diamantane would then be given by $C_{dia} = f_{gb}\ \rho_{dia}/2\rho_{Al}$ where ρ_{dia} and ρ_{Al} are the densities of diamantane and Al, respectively. Taking $\rho_{dia} = 1.2$ g/cm^3 and $\rho_{Al} = 2.7$ g/cm^3, an addition of diamantane for the desired dispersion of diamantane molecules on the grain boundaries is estimated to be 0.9% by weight. Accordingly, a 1 wt% addition of diamantane was used in the present study.

Nanocrystalline Al with 1 wt% diamantane was produced by mechanical milling a slurry of both commercial purity (99.9%) Al and diamantane powder in liquid nitrogen (cryomilling)). A detailed description of the cryomilling process used is given elsewhere [22]. The present cryomilling was performed in a modified Union Process 01-HD attritor with a stainless steel vial at a rate of 180 rpm. Stainless steel balls (6.4 mm diameter) were used with a ball-to-powder weight ratio of 32:1. During the milling operation that lasted for 8 h, liquid nitrogen was added directly into the mill to maintain complete immersion of the milling media. Prior to milling, approximately 0.2 wt% stearic acid [$CH_3\ (CH_2)_{16}CO_2H$] was added to the powders as a process control agent to prevent adhesion of the powders to the milling tools during the process. The experimental conditions in this study were kept as close as possible to the study of Zhou et al. [15] which was conducted in the same cryomilling facility, to be able to compare the present results with theirs for cryomilled Al without the addition of diamantane. The milling container and aluminum powders used in this study were also the same as those for the previous study of Zhou et al. [15]. Prior to and following cryomilling, scanning electron microscopy (SEM) was performed using a FEI/Philips XL-30 microscope to determine the average particle size and general particle morphology of each sample. Standard chemical analysis of the as-milled powders was also conducted according to ASTM E 1019-08, ASTM E 1097-07, and ASTM E 1447-09.

Samples of the cryomilled Al + 1% diamantane powder were sealed in glass tubes in an inert atmosphere of Ar gas to avoid oxidation and contamination. The samples were

then annealed in a Cress C-601K resistance furnace at 423, 473, 523, 573, 623, 673, 698, 723, 748, or 773 K, for times ranging from 0.5 to 10 h to test the thermal stability of the grains. The thermal exposures were limited to 773 K due to the potential for incipient melting of the Al above this temperature.

The as-cryomilled and thermally exposed powder samples were each examined using transmission electron microscopy (TEM). TEM sample preparation consisted of suspending the nanostructured powders in methanol, agitating the solution by hand, and submersing a Cu TEM grid into the methanol where the powders adhered to it. Micrographs of the powders were produced using a Philips CM20 transmission electron microscope operated at 200 kV. Average grain size was determined directly from the TEM micrographs by measuring the diameters of 500 grains for each sample using ImageJ image analysis software (National Institutes of Health). Bright-field TEM images were used for this grain size determination following the procedures of Zhou et al. [15]. Dark-field TEM images were also produced and used to confirm the measurements made with bright-field images. Although the boundaries were occasionally sharper on the dark-field images, no difference in grain size was observed. As a further confirmation of the TEM results, X-ray diffraction (XRD) measurements were also performed with a Siemens D5000 diffractometer equipped with a graphite monochromator using Cu K_α radiation ($\lambda = 0.1542$ nm) at 100 steps per degree and a count time of 8 s per step. Following subtraction of the instrumental broadening and $K_{\alpha 2}$ components, full width half maximum (FWHM) line broadening for five prominent face-centered-cubic (FCC) Al peaks (111, 200, 220, 311, 222) was measured for an additional assessment of the grain size in the Al + 1% diamantane samples.

Gas chromatography–mass spectrometry (GC–MS) analysis was performed to qualitatively determine the presence of diamantane in the cryomilled aluminum matrix. First, the cryomilled aluminum was washed with heptane to remove any free diamantane on the surface. The cleaned powders were then mixed with concentrated nitric acid to dissolve the Al matrix and release diamantane particles that were embedded in the Al matrix into the acid solution. Heptane was then added to the acid solution to extract the diamantane. A Trace MS^+ GC–MS (Thermo) was used to detect diamantane extracted from the cryomilled aluminum. The GC column had dimensions of 30 m × 0.32 mm ID DB-5. The GC oven was programmed to start at a temperature of 323 K and ramp at 10 K/min to 563 K. Spectra were obtained using electron ionization with a mass (m/z) range of 50–650.

Results

The morphological change of the Al + 1% diamantane powders during cryomilling was similar to that for pure Al produced in an earlier study [15]. For example, the shapes of the particles, which look spherical in the as-received sample with a particle size range of 17–35 μm (Fig. 1a), become smaller and polygonal after 8 h of cryomilling (Fig. 1b). However, the average particle size of Al + 1% diamantane after cryomilling was smaller than that observed for cryomilled Al without diamantane additions by about a factor of two with an average diameter of 13 μm.

Figure 2 shows the XRD spectra of cryomilled Al + 1% diamantane and cryomilled Al [15]. Comparing the peaks of the two spectra, it can be seen that no shift in the peak position or peak broadening occurred as a result of the diamantane addition. Thus, the presence of the diamantane produced little or no lattice strain in the aluminum matrix and the grain size of cryomilled Al + 1% diamantane should be essentially same as that for Al cryomilled without the diamantane addition. Both of these findings are

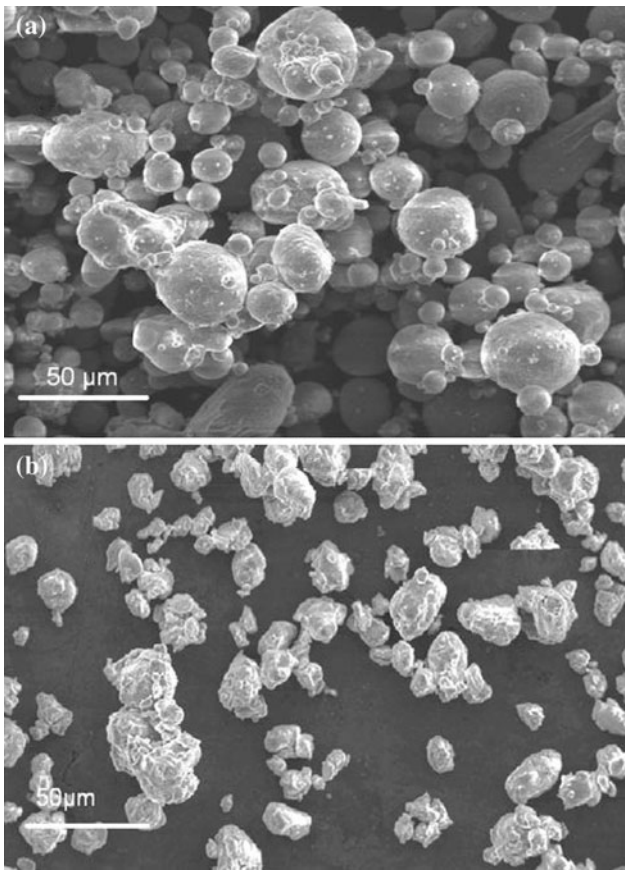

Fig. 1 SEM secondary electron images of **a** as-received Al powders and **b** Al + 1% diamantane powders that were produced by cryomilling for 8 h

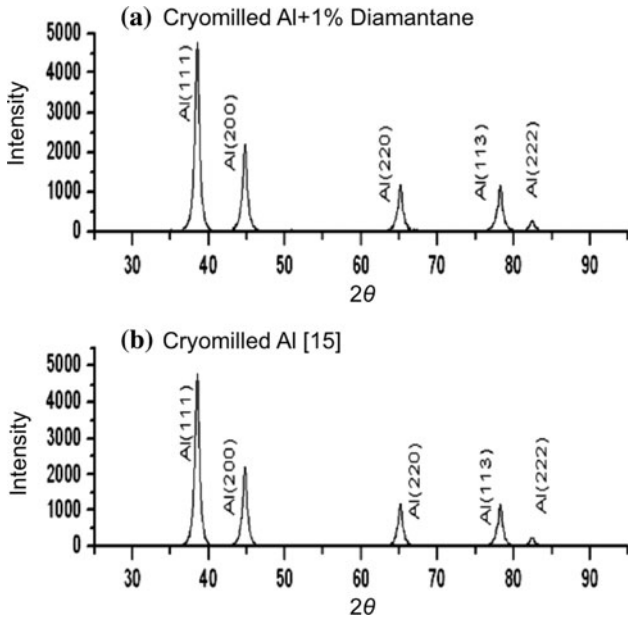

Fig. 2 XRD spectra comparing the peaks obtained for **a** cryomilled Al + 1% diamantane and **b** cryomilled Al [15]

supported by estimating lattice strain using the integral breadth method and by measuring grain size using TEM micrographs as well as XRD techniques. Measurements based on TEM images indicated that the average grain size for cryomilled Al + 1% diamantane was about 22 nm, with a standard deviation of 6 nm ($N = 500$) and essentially the same as the average grain size value of 26 nm determined for cryomilled pure Al that does not contain diamantane [15].

A TEM bright-field image of cryomilled Al + 1% diamantane alloy at higher magnification indicating nano-sized grains (<100 nm) is presented in Fig. 3. A histogram of the grain size distribution for the present Al + 1% diamantane alloy is illustrated in Fig. 4 which exhibits a single mode that is approximately equal to the mean. XRD measurements of average grain size values were of the

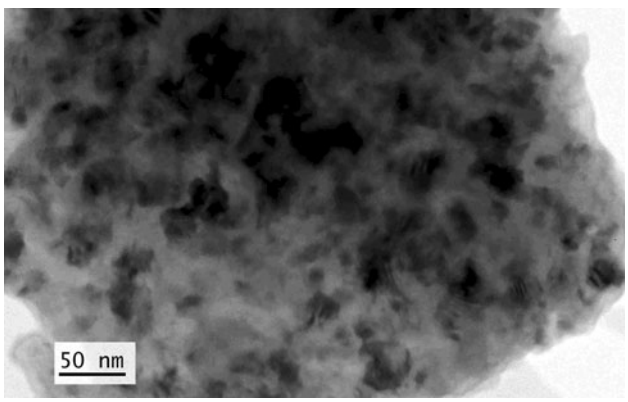

Fig. 3 TEM micrograph of as-cryomilled Al + 1% diamantane

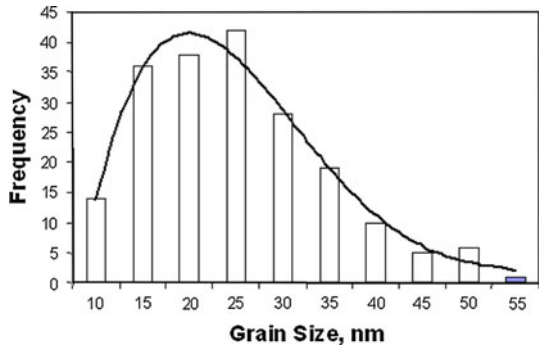

Fig. 4 Grain size distribution for cryomilled Al + 1% diamantane

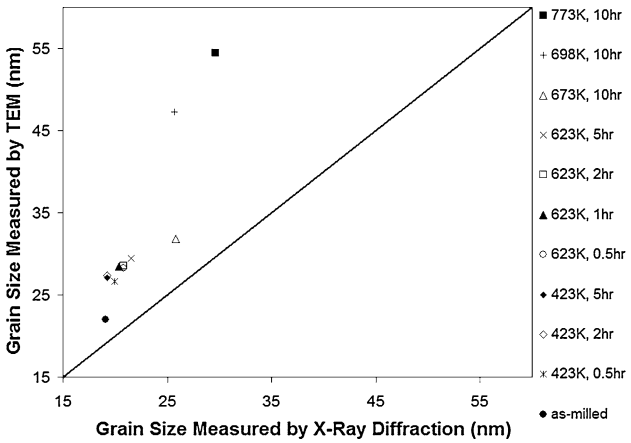

Fig. 5 Comparison of grain size for thermally treated cryomilled particles determined from TEM micrographs and XRD peak width measurements

same order of the grain size values determined from TEM micrographs but on average were about 32% smaller as illustrated in Fig. 5. Accordingly, grain size values determined from TEM are reported in the following as the more conservative estimates. It is also evident that the TEM measurements are more consistent with the thermal exposure durations and temperatures employed.

Grain size versus annealing time is plotted for cryomilled Al + 1% diamantane and compared with that for cryomilled pure Al in Fig. 6 [15]. The thermal exposure temperature ranged from 473 to 773 K for pure Al ($0.51T_m$ to $0.83T_m$, where T_m is the melting temperature of Al) for durations of up to 3 h. For this study, a broader temperature range was employed ($0.45T_m$ to $0.83T_m$) as well as thermal exposures of as long as 10 h. The standard deviations for the average grain size values in Fig. 6 range from 4.2 to 8.7 nm. The data in this figure reveal four findings for Al + 1% diamantane: (i) the increase in grain size with temperature is relatively small; (ii) the growth rate decreases with increasing exposure time at a given temperature; (iii) significant grain growth is only observed at temperatures greater than 698 K; and (iv) even at the

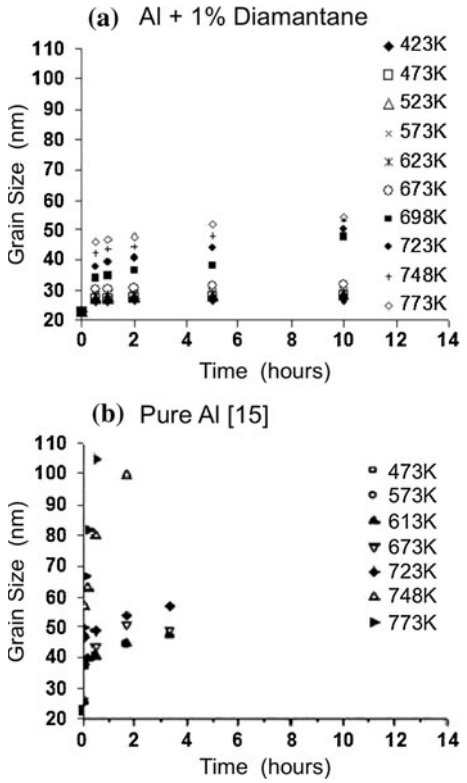

Fig. 6 Grain size as a function of annealing time at various temperatures for cryomilled **a** Al with the addition of 1% diamantine, and **b** pure Al [15] for comparison

highest temperatures the grain size remained well below 100 nm.

It appears from the measurements in Fig. 6 that there are a significant number of grains that undergo limited growth during the first 2 h of thermal exposure. This relatively early growth may correspond to recovery of some boundaries, a phenomenon that facilitates the reduction of stored energy by the removal or rearrangement of dislocations [23]. The observation of low angle boundaries in the as-cryomilled powders and their apparent absence in all the present specimens that were heated lends support to this hypothesis. By contrast, substantially more grain growth occurs during the first 2 h for pure Al (Fig. 6b). This finding is particularly apparent for temperatures greater than 573 K where the average grain size reaches the range of 50–100 nm.

TEM micrographs of Al + 1% diamantane annealed for 1 and 10 h are presented in Fig. 7 for 423 K, and also in Fig. 8 for 1 and 10 h at 773 K. For relatively low temperatures (e.g., 423 K), visual inspection of TEM micrographs reveals no obvious increase in grain size even after annealing for l0 h as demonstrated in Fig. 7. A similar trend is also observed for the highest temperatures (e.g., 773 K) as demonstrated in Fig. 8.

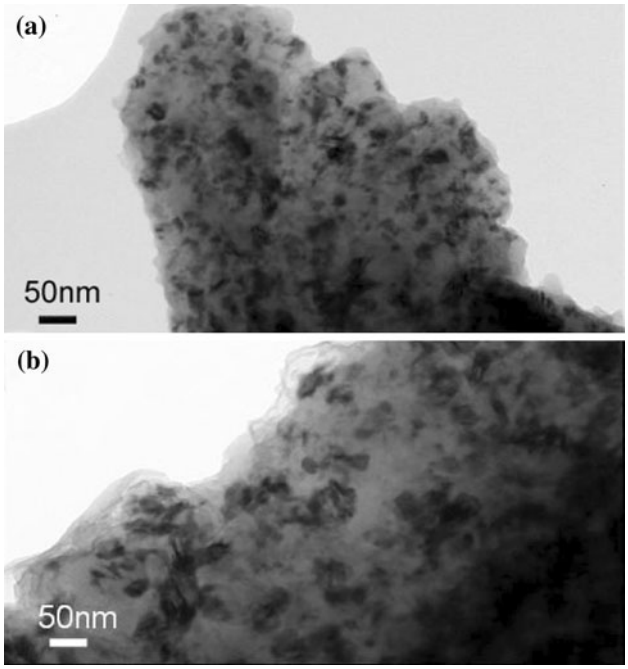

Fig. 7 TEM bright-field image of cryomilled Al + 1% diamantane alloy annealed at 423 K for **a** 1 h and **b** 10 h

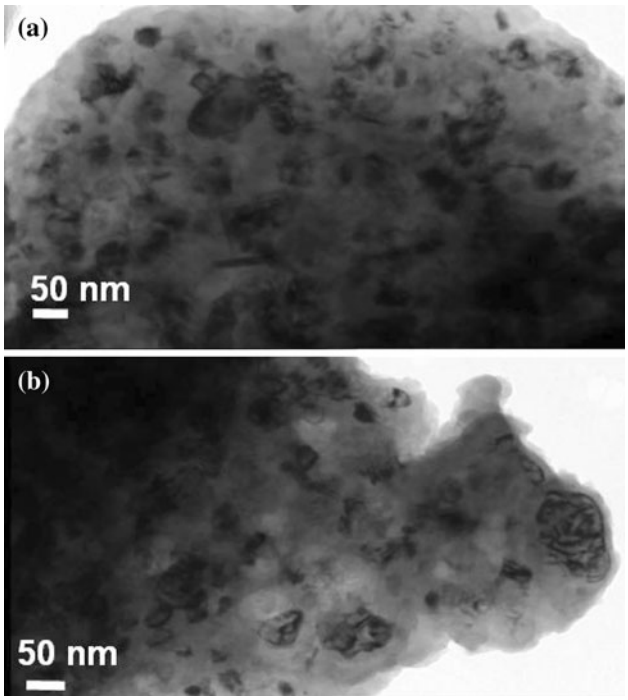

Fig. 8 TEM bright-field image of cryomilled Al + 1% Diamantane alloy annealed at 773 K for **a** 1 h and **b** 10 h

The present observations clearly indicate superior grain size stability for Al + 1% diamantane alloy over cryomilled pure Al. Specifically, the grain size for Al + 1% diamantane is less than that for cryomilled Al over the entire temperature range by about a factor of two. Perhaps,

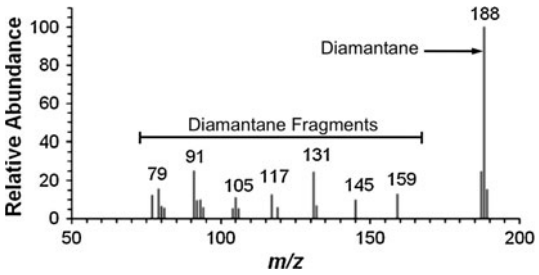

Fig. 9 GC mass spectrum indicating the presence of diamantane for the extraction solution obtained from the present cryomilled aluminum powders (retention time = 12.9 min)

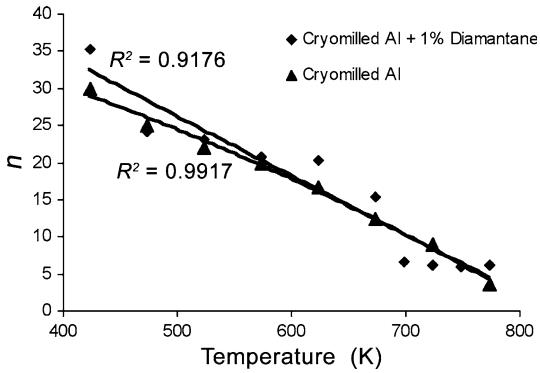

Fig. 10 Grain growth exponent, n, as a function of annealing temperature for cryomilled pure Al and Al + 1% diamantane. Correlation coefficient values corresponding to the linear regression fits to the data for each material are indicated

most notable is that the grain size remains in the nanometer range (<100 nm) at even the highest temperatures corresponding to $0.78T_m$ to $0.83T_m$ while, in the absence of diamantane, a grain size of 100 nm is exceeded for temperatures above 723 K [15]. A similar lack of thermal stability was observed for cryomilled 5083 Al–Mg at temperatures above 654 K [24].

The diamantane extraction solution from the present cryomilled alloy was analyzed using GC–MS. A peak at a retention time of 12.9 min was observed in the gas chromatograph of the extraction solution that was found to correspond to diamantane. The mass spectrum for this retention time is shown in Fig. 9. This spectrum for the extraction solution exhibits the molecular ion at *m/z* 188 and characteristic fragments for diamantane that are in excellent agreement with the Wiley Mass Spectrometry Library values for diamantane as well as the spectrum for pure diamantine when it was tested separately. Thus, GC–MS analysis unambiguously confirmed the presence of diamantane embedded in the matrix of the present cryomilled Al powders.

Discussion

Grain growth in conventional polycrystalline materials is normally controlled by atomic diffusion along grain boundaries. This process has been frequently represented by the following empirical equation [25, 26]:

$$d^n - d_0^n = kt, \tag{2}$$

where d is the average instantaneous grain diameter, d_0 is the initial grain size, t is the annealing time, n is the grain growth exponent, and k is a parameter that depends on temperature. The elementary theories of grain growth, predict a value of 2 for n for very pure metals or at high temperatures. However, experimental data have indicated that the value of n is significantly >2 in most cases, and that it generally decreases with increasing temperature, approaching a lower limit of 2 for very pure metals or at very high temperatures. For example, n ranged from a value of 20 at low temperatures and decreased to about 3 at higher temperatures for grain growth in nanocrystalline Fe powder [27]. Differentiating Eq. 2 yields a relation for the isothermal rate of grain growth of the form

$$\dot{d} = \frac{k}{n}\left(\frac{1}{d}\right)^{n-1} \tag{3}$$

The value of n was estimated from a correlation based on Eq. 3. The resultant values of the grain growth exponent, n, for cryomilled Al + 1% diamantane are plotted against thermal exposure temperature in Fig. 10. The corresponding value of n for cryomilled pure Al [15] is also shown in the same graph for comparison. Figure 10 reveals that the grain growth exponent, n, decreases for both materials with increasing temperature, a trend that has been reported for other alloys processed by cryomilling [26]. We note that the value of n is always greater than two for the present powders. Overall, the value of n for Al + 1% diamantane is consistently only slightly greater than that for cryomilled pure Al up to 673 K.

Zhou et al. [15] pointed out that a value of n greater than two can result from Zener pinning of the grain boundaries by particles. They proposed that this pinning results from the presence of nanoscale nitride particles that are a byproduct of the cryomilling process. For this study, it follows that additional pinning could be facilitated by diamantane nanoparticles at the grain boundaries.

Table 1 lists the chemical composition of the as-cryomilled Al + 1% diamantane alloy powders together with the composition for Al powders reported in [15]. The concentrations of impurities in the present alloy are similar to those for cryomilled pure aluminum with the exception of a five-fold greater concentration of C that can be attributed to the diamantane addition. Further, it is unlikely that the greater amount of C observed could be due to the

Table 1 Chemical composition (in wt%) of cryomilled Al + 1 wt% diamantane

Sample	C	N	O	H	Fe	Cr	Mn
Al + 1% diamantane	1.25	0.26	0.89	0.24	0.13	0.007	0.002
Al (Zhou et al. [15])	0.26	0.25	0.85	NR	0.15	0.013	0.003

The composition for cryomilled pure Al is also listed for comparison

NR not reported

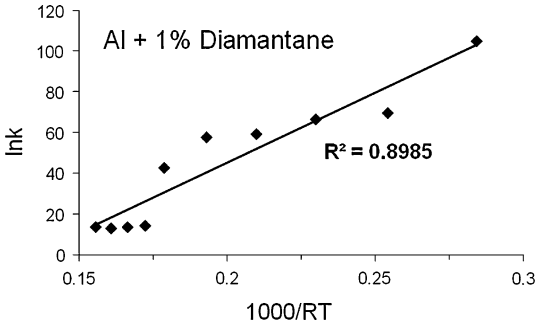

Fig. 11 Values of ln(k) versus 1000/RT based on Eq. 5 for grain growth by simple diffusion

use of stearic acid since the same amount of stearic acid was used in an identical procedure for pure Al [15] as that used in this study. Accordingly, the greater carbon content compared to that for pure Al can be attributed to the incorporation of diamantane. This assertion is reinforced by a measurable amount of hydrogen in the present as-milled powder that was not reported by Zhou and colleagues. The presence of both C and H resulting from the addition of the diamantane leads to three possibilities: (a) the formation of Al carbide particles during milling that provide a drag force, (b) the segregation of H and C to boundaries, a process that could also retard boundary mobility, and (c) a stable dispersion of diamantane exists at the grain boundaries as a result of cryomilling.

Activation energy, Q, has often been used to identify the microscopic mechanism that dominates grain growth. The rate constant k in Eq. 3 can be expressed by the Arrhenius equation

$$k = k_0 \exp\left(\frac{-Q}{RT}\right), \tag{4}$$

where Q is the activation energy for the grain growth, k_0 is a constant that is assumed to be independent of the temperature and time, R is the molar gas constant, and T is temperature. The values of k for different annealing temperatures can be determined using the values of n and the values of k/n from the slopes and the intercepts, respectively, of linear fits to the data. The natural logarithm of k in Eq. 4 is plotted versus 1000/RT in Fig. 11 such that the slope of this plot corresponds to the value of the activation energy. As indicated by Fig. 11, the data fit a curve with positive slope implying untenable negative activation energy. In addition, the observation that the grain size exponent, n, inferred from Fig. 10 is >2 suggests the operation of strong pinning forces on boundaries. Thus, another model that takes into account pinning forces is needed to reasonably predict the present grain growth data.

Burke [17] proposed such a model in which pinning forces govern grain growth in the presence of a dispersion of particles. According to this treatment, the grain growth rate is not controlled solely by the instantaneous grain size, d, but rather by the decreasing difference between an ultimate limiting grain size, d_m, and the changing value of the instantaneous grain size. For a given temperature, the relation between grain size and time based on Burke's model may be expressed by

$$\frac{d_o - d}{d_m} + \left(\frac{d_m - d_o}{d_m - d}\right) = \frac{t}{d_m} k_0 \exp\left(\frac{-Q}{RT}\right) \tag{5}$$

This treatment assumes that the drag force is independent of grain size. As shown by Michels et al. [28], such an assumption is reasonable under the condition that the source of pinning does not depend on grain size. This situation exists when a dispersion particles or pores produce the pinning forces. Differentiating Eq. 5 gives the following grain growth rate equation:

$$\dot{d} = k_0 \exp\left(\frac{-Q}{RT}\right)\left(\frac{1}{d} - \frac{1}{d_m}\right) = k\left(\frac{1}{d} - \frac{1}{d_m}\right) \tag{6}$$

Figure 12 shows ln(k), determined using Eq. 6, plotted as a function of 1000/RT. Distinctly different activation energies are indicated for two temperature regimes in this figure. Grain growth data for cryomilled CP Al and Al alloy 5083 in powder [15, 22] and bulk form [18] reported previously in the literature have also indicated two different activation energies associated with grain coarsening in these cryomilled Al alloys. Figure 12 demonstrates characteristics similar to those for other cryomilled Al alloys: an elevated temperature region that corresponds to relatively high activation energy and a lower temperature region characterized by relatively low value of the activation energy. The activation energies and the corresponding transition temperature between them for cryomilled Al alloys studied previously [15, 18, 24] as well

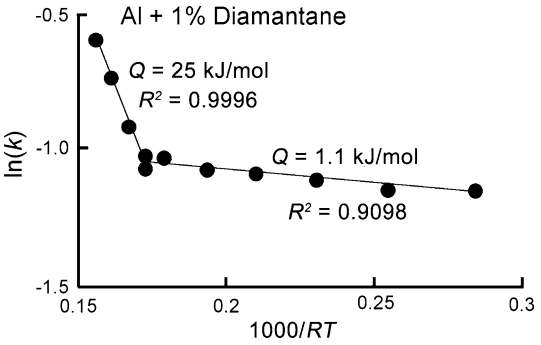

Fig. 12 Arrhenius plot of ln(k) as a function of 1000/RT for grain growth inhibited by dispersion particle drag revealing high- and low-temperature regimes of behavior

as the present material containing diamantane are compared in Table 2.

The activation energy for grain boundary diffusion (86 kJ/mol) and lattice diffusion (143.4 kJ/mol) reported for polycrystalline aluminum [28] are both well above the 25 kJ/mol observed for Al + 1% diamantane in the higher temperature regime ($T > 673$ K). Others proposed previously that the two regimes of behavior identified in Table 2 are associated with relaxation processes at lower temperatures and grain growth processes at the higher temperatures [18]. However, the relatively low activation energy for the higher temperature behavior observed in this study is closer in value to that for the lower temperature behavior of cryomilled pure Al and Al alloys [15, 18, 24]. As shown in Table 2, the activation energy in the higher temperature regime for Al + 1% diamantane is essentially the same as that observed in the lower temperature regime for cryomilled 5083 Al alloy [18]. Based on comparisons of grain growth activation energy with those for other processing routes, they attributed this relatively low activation energy to processes associated with the reordering of non-equilibrium grain boundaries [18]. This process may also be facilitating the grain growth for Al + 1% diamantane based on a similar value of the activation energy but for the higher temperatures employed.

The present activation energy for the lower temperature regime ($T < 673$ K) is extremely small at 1.1 kJ/mol. As shown in Table 2, this value is somewhat below the activation energy of 5.6 kJ/mol determined by Tellkamp et al. [24] for cryomilled 5083 Al alloy in this temperature regime. No mechanism was suggested to explain the low activation energy observed for this alloy, although recrystallization was ruled out [24]. We postulate that the present lower temperature regime of behavior may be associated with stress relaxation facilitated by less stable processes such as recovery of dislocation segments or sub-boundary remnants. This hypothesis is based on residual stresses within the nanostructure that can result from non-uniform severe deformation that occurs during cryomilling. Grain growth associated with stress relaxation is also consistent with the fact that the majority of the grain growth at the lower temperatures took place within the first 30 min of thermal exposure. We would expect grain growth driven by relaxing stresses would be most rapid initially and quickly arrest as stresses are relaxed below a threshold level.

Sufficiently elevated residual stresses could also be relaxed by a stress-driven grain growth process that has been observed in nanocrystalline Al thin films at ambient temperatures [29]. This mechanism has been attributed to grain boundary shear-migration coupling that occurs under stresses that approach or exceed the yield stress [30]. Although residual stresses resulting from cryomilling are probably somewhat lower than this level, they could be sufficient for driving grain growth at the temperatures employed in the present thermal exposure experiments.

We note that adding diamantane molecules to aluminum during cryomilling stabilizes the grain size beyond that achieved with the nitrides and other nanoscale particles that naturally occur when cryomilling Al and Al alloys [14–16, 31]. This added stability could be due to the fact that diamantane has a relatively small diameter of about 2 nm when compared to other dispersoids that are added to NC-Al [31]. We also chose a diamantane concentration that could lead to particle spacing that is on the order of the diameter of the diamantane molecules themselves

Table 2 Grain growth activation energies determined for cryomilled Al alloys

Authors	Materials	Transition temperature (K)	Q_H (kJ/mol)	Q_L (kJ/mol)
Roy et al.[a]	Al5083 consolidated cryomilled alloy	523	110	25
TellKamp et al.[b]	Al5083 cryomilled powders	654	142	5.6
Zhou et al.[c]	Pure Al cryomilled powders	723	112	79
This study	Al + 1% diamantane cryomilled powders	673	25	1.1

[a] Reference [18]

[b] Reference [24]

[c] Reference [15]

according to Eq. 1. This smaller size and spacing of the diamantane would allow for stronger effect on the migration of grain boundaries in a manner similar to Orowan strengthening by the interaction of dislocations with a dispersion of particles. By the same token, it is doubtful that the particle sizes and spacings observed for other cryomilled NC Al alloys that are on the order of or larger than the grain size would have as strong an interaction with grain boundary migration. More research is required to better understand nanoparticle–grain boundary interactions that can account for the profoundly limited grain growth observed in this study.

Conclusions

Commercially pure aluminum powders were cryomilled with 1 wt% diamantane for 8 h producing mechanically alloyed powders with an average grain size of 22 nm. This material exhibited greater thermal stability than cryomilled pure Al in the temperature range of 423 to 773 K ($0.45–0.83T_m$). Specifically, the grain size of cryomilled Al + 1% diamantane was consistently found to be less than half of that for cryomilled pure Al under the same thermal exposure conditions. The grain size remained nanocrystalline (<100 nm) for Al + 1% diamantane, even after 10 h at the highest temperature of 773 K.

Analysis of grain size data from the thermal exposure experiments indicated that diffusive grain growth theory could not account for the observed behavior. Rather, the value of the grain growth exponent and the sharp deceleration in grain growth observed suggested that the operation of strong pinning forces on the boundaries during thermal exposure. Accordingly, the Burke model for grain growth inhibited by drag forces exerted by a dispersion of particles was applied to the present data. As observed for other cryomilled Al alloys, two grain growth regimes were identified using this model: one at relatively low temperatures (423–673 K) where the activation energy is approximately 1.1 kJ/mol and another at higher temperatures where the activation energy is about 25 kJ/mol. Neither of these values corresponds to grain growth by diffusion since the activation energy for this process in Al is substantially greater. Other processes such as stress relaxation by grain boundary reordering, shear-migration coupling, and annealing of dislocation segments or subboundary remnants are possible candidates. More study is needed to clearly identify the processes responsible for the relatively low level of grain growth observed.

Acknowledgements This study was supported by the National Science Foundation (Grant No DMR-0702978) and the UC Discovery Program with matching support from the Boeing Company (Award No. GCP07-10250). The authors wish to also acknowledge assistance from Dr. W. A. Chiou of the Univ. of Maryland, Dr. J. Greaves of the UC Irvine Mass Spectrometry Facility as well as Gloria Chow and Dr. Robert Carlson of ChevronTexaco Technology Ventures, LLC for their generous assistance in this study.

References

1. Suryanarayana C (1995) Int Mater Rev 40:41–64
2. Witkin DW, Lavernia EJ (2006) Prog Mater Sci 51:1
3. Gleiter H (2000) Acta Mater 48:1
4. Birringer R, Gleiter H, Kelien HP, Marquardt P (1984) Phys Lett A 102:356
5. Inoue A (1994) Mater Sci Eng A 179–180:57
6. Hughes GD, Smith SD, Pande CS, Johnson HR, Armstrong RW (1986) Scripta Metall 20:93
7. Li ZG, Smith DJ (1989) Appl Phys Lett 55:919
8. Lu K, Wang JT (1991) J Appl Phys 69:522
9. Mandich ML, Bondybey VE, Reents WD (1987) J Chem Phys 86:4245
10. Segal VM, Reznikov VI, Drobyshevskiy AE, Kopylov VI (1981) Metally 1:11523
11. Koch CC (1997) Nanostruct Mater 9:13
12. Fecht HJ (1995) Nanostruct Mater 6:33
13. Shewmon PG (1969) Transformation in metals. McGraw-Hill, New York
14. Perez RJ, Jiang HG, Dogan CP, Lavernia EJ (1998) Metall Mater Trans A 29A:2469
15. Zhou F, Lee J, Dallek S, Lavernia EJ (2001) J Mater Res 16:3451
16. Hofmeister C, Yao B, Sohn YH, Delahanty T, van den Bergh M, Cho K (2010) J Mater Sci 45:4871. doi:10.1007/s10853-010-4571-8
17. Burke JE (1949) Trans TMS-AIME 180:73
18. Roy I, Chauhan M, Lavernia EJ, Mohamed FA (2006) Metall Mater Trans A 37A:721
19. Dahl JE, Liu SG, Carlson RMK (2003) Science 299:96
20. Yamasaki T (2000) Mater Phys Mech 1:127
21. Choi D, Kim H, Nix WD (2004) IEEE J Microelctromech Syst 13:230
22. Luton MJ, Jayanth CS, Disko MM, Matras S, Vallone J (1989) Mater Res Soc Symp Proc 132:79
23. Mohamed FA (2003) Acta Mater 51:4107
24. TellKamp VL, Dallek S, Cheng D, Lavernia EJ (2001) J Mater Res Soc 16:938
25. Benjamin JS, Volin TE (1974) Metall Trans A 5:1929
26. Beck PA, Towers J, Manly WD (1947) Trans TMS-AIME 175:162
27. Malow TR, Koch CC (1997) Acta Mater 45:2177
28. Michels A, Krill CE, Ehrhardt H, Birringer R, Wu DT (1997) Acta Mater 47:2143
29. Legros M, Gianola DS, Hemker KJ (2008) Acta Mater 56:2253
30. Caillard D, Mompiou F, Legros M (2009) Acta Mater 57:2390
31. Han BQ, Ye J, Tang F, Schoenung J, Lavernia EJ (2007) J Mater Sci 42:1660. doi:10.1007/s10853-006-0907-9